Main inductances of induction motor for diagnostically specialized mathematical models

TOMASZ WĘGIEL, KONRAD WEINREB, MACIEJ SUŁOWICZ

Department of Electrical and Computer Engineering
Cracow University of Technology, Cracow, Poland
e-mail: pewegiel@cyfronet.pl

Abstract: In the paper modeling of main inductances for mathematical models of induction motors is applied to study the effects caused by a rotor eccentricity and saturation effects. All three possible types of eccentricity: static, dynamic and mixed are modeled. The most important parameters describing rotor eccentricity include self and mutual inductances of the windings. The structural changes of the permeance function as a result of eccentricity appearance and the Fourier spectra of inductances in occurrence of saturation for each case are determined in the paper. The presented algorithm can be used for the diagnostically specialized models of induction motors.

Key words: induction motors, rotor fault diagnosis, rotor eccentricity

1. Introduction

The usefulness of the circumferential mathematical models of electrical machines using electromagnetic field for energy transformation is conditioned by the simplicity of determining the parameters of the model equations. In circuit models the winding distributions and the rotor air-gap geometry are usually represented by the inductances of the motor windings [1, 2]. Then, a determination of inductances is the first and necessary step of modeling [3-10].

The problem of the determination of inductances for symmetrical machines has been researched extensively for years and was thoroughly discussed in the literature. The problem becomes more difficult when the symmetry of the magnetic circuit is damaged, what happens for example when the stator and the rotor loose the axial position. Therefore, this paper subjects are study of effects due to the rotor eccentricity for a cage induction motor [11-13].

The determination of inductances using field methods require tedious and time consuming calculations. In this paper a simple but very effective method of solving this problem, based on the so called concept of "sinusoidal" windings [1] was used.

In order to calculate winding inductances, their MMFs and the permeance function of the air-gap are required. Influence of saturation effects and slotting on both sides of the air-gap change the permeance function essentially and make calculation of inductances a little bit sophisticated.

The methods of determining the linear permeance function are based on geometrical dependencies in reference to the air-gap dimension, previously described in [14-17] but it requires correction due to the saturation. This modification consists of making the permeance a function of the air-gap flux position and amplitude. This problem of saturation was described in [18], wherein the main concerns of the authors were the prediction of the air-gap length as a function of magnetizing current for case of stator and rotor symmetry. Generally these models are developed from the models with linear magnetic circuits, where saturation is introduced, is based on assumption of a sinusoidally distribution windings and symmetry of air-gap. Another approach to determine the air-gap flux density components for saturated machines is described in [19]. The modeling of saturation by the variable permeance of air-gap was also presented in [20, 21].

In this paper a new approach to modeling the inductance coefficients for induction motors is developed, where known [18] assumptions are made to transform the linear inductances into the nonlinear one, however, for motor with rotor eccentricities.
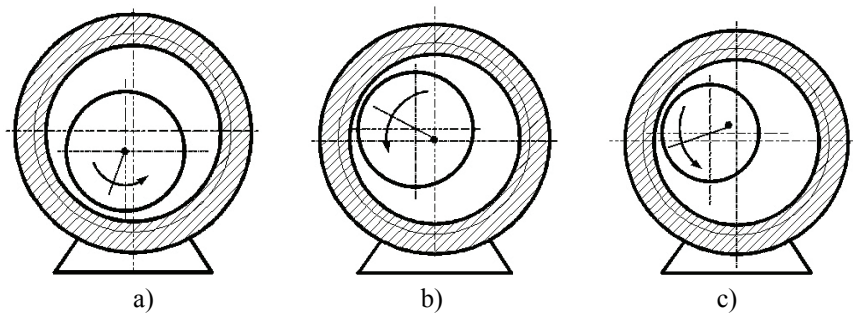

Fig. 1. Simplified cross-sections of motors with eccentricities: a) static; b) dynamic; c) mixed

Three types of eccentricity are distinguished:
-   **static**, when the rotor rotation axis coincides with the rotor symmetry axis $0r$ but does not with the stator symmetry axis $0s$,
-   **dynamic**, when the rotor rotation axis coincides with the stator symmetry axis $0s$ but does not with the rotor symmetry axis $0r$,
-   **mixed**, when the rotor rotation axis does not coincide both with the rotor symmetry axis $0r$ and with the stator symmetry axis $0s$.

A detailed analytical algorithm of a new method modeling the inductance coefficients for induction motors is presented. The resulting can be used in mathematical models of induction motor created for diagnostic purpose.

2. Changes of air-gap permeance function to eccentricity and saturation

The permeance function of the air-gap is an inverse of the length of magnetic field force lines in the air-gap [14]

$$\Lambda(x,\varphi) = \frac{1}{\delta_c(x,\varphi)} \; .$$

(1)

It can be precisely found from magnetic field distribution in the air-gap or it can be determined approximately. In this paper, the permeance function has been determined by simplified method from the air-gap geometry. Firstly, a function of a magnetic field line length in the air-gap along circumference has been approximately found.

Fig. 2. Simplified cross-section of a motor explaining types of eccentricities
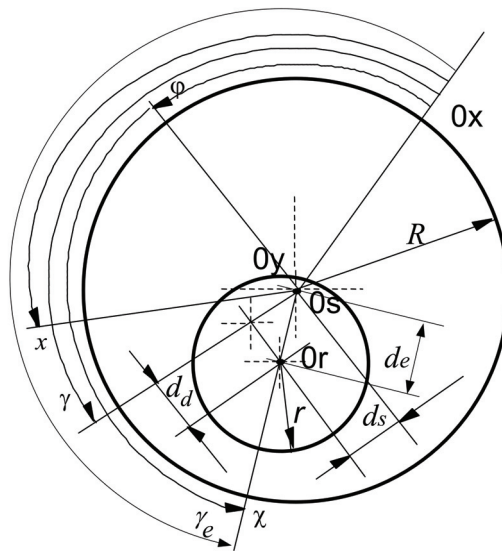
Parameters d_e and γ_e in Fig. 2 are determined by parameters given as follow
– for static eccentricity

$$d_e = d_s, \quad d_d = 0, \quad \gamma_e = \gamma = \text{const} ,$$

(2)

– for dynamic eccentricity

$$d_e = d_d, \quad d_s = 0, \quad \gamma_e = \varphi + \chi ,$$

(3)

– for mixed eccentricity

$$d_s \neq 0, \quad d_d \neq 0, \quad \gamma = \text{const},$$

$$d_e = d(\varphi) = \sqrt{d_s^2 + d_d^2 + 2 d_s d_d \cos(\varphi - \gamma)} ,$$

(4)

$$\gamma_e = \arcsin\left(\frac{d_d}{d_e} \sin(\varphi - \gamma) \right) \qquad \text{for} \quad d_e \neq 0.$$

The level of eccentricities is represented by formulas: $\varepsilon_s = d_s / \delta$, $\varepsilon_d = d_d / \delta$, where $\delta = R - r$.
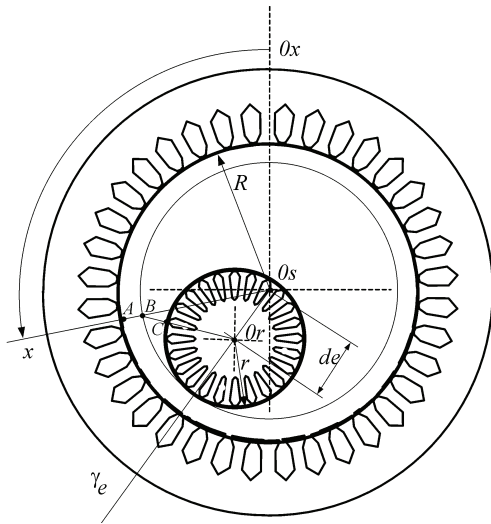
Fig. 3. An approximation of magnetic field lines in the air-gap

Good results for a smooth air-gap can be obtained using the approach, which keeps perpendicular crossing of the boundary between iron and air by magnetic field force lines. The length of a magnetic field force line in the air-gap is equal to the sum of segments AB and BC in Fig. 3 and is given by the formula

$$\delta(x,\varphi) = R - 2r - d_e + \sqrt{\left[(r+d_e)\cos x - d_e \cos \gamma_e\right]^2 + \left[(r+d_e)\sin x - d_e \sin \gamma_e\right]^2} \ . \qquad (5)$$
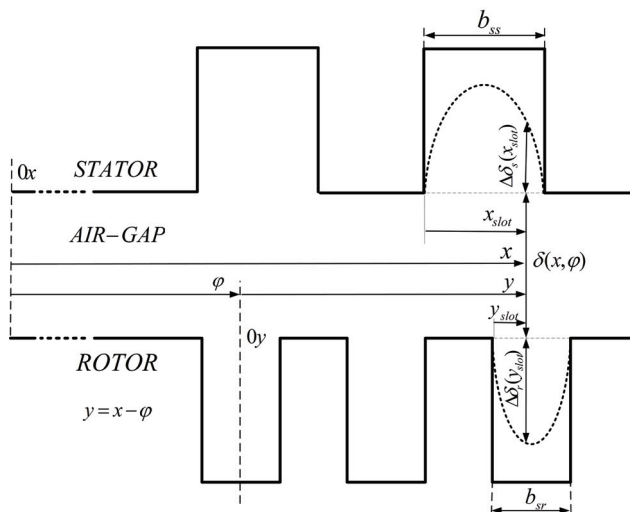

Fig. 4. Explanation to calculations of correction values

The slots on the stator and the rotor sides modify locally this length. Then, correction values $\Delta\delta_s(x)$ and $\Delta\delta_r(y)$ should be added in respective places.

$$\delta_0(x,\varphi) = \delta(x,\varphi) + \Delta\,\delta_s(x) + \Delta\delta_r(y).$$ (6)

These slots corrections can be determined using the conformal mapping approach as it is done for field calculations in a slot similar to Carter coefficient determination [14]

$$\Delta\delta_s(x) = \begin{cases} 0 & \text{for stator teeth} \\ \Delta\delta_{max}^s(x)\,\sin\left(\dfrac{\pi}{b_{ss}}x_{slot}\right) & \text{for stator slots,} \end{cases}$$ (7)

$$\Delta\delta_r(y) = \begin{cases} 0 & \text{for rotor teeth} \\ \Delta\delta_{max}^r(y)\,\sin\left(\dfrac{\pi}{b_{sr}}y_{slot}\right) & \text{for rotor slots,} \end{cases}$$ (8)

where:

$$\Delta\delta_{max}^s(x) = \delta(x,\varphi)\,\frac{\left(\dfrac{b_{ss}}{2\delta(x,\varphi)} + \sqrt{1 + \left(\dfrac{b_{ss}}{2\delta(x,\varphi)}\right)^2} - 1\right)^2}{2\left(\dfrac{b_{ss}}{2\delta(x,\varphi)} + \sqrt{1 + \left(\dfrac{b_{ss}}{2\delta(x,\varphi)}\right)^2}\right)},$$ (9)

$$\Delta\delta_{max}^r(y) = \delta(x,\varphi)\,\frac{\left(\dfrac{b_{sr}}{2\delta(x,\varphi)} + \sqrt{1 + \left(\dfrac{b_{sr}}{2\delta(x,\varphi)}\right)^2} - 1\right)^2}{2\left(\dfrac{b_{sr}}{2\delta(x,\varphi)} + \sqrt{1 + \left(\dfrac{b_{sr}}{2\delta(x,\varphi)}\right)^2}\right)},$$ (10)

b_{ss} is an equivalent stator slot opening,
x_{slot} is a local variable over a stator slot; $x_{slot} \in (0,\ b_{ss})$,
b_{sr} is an equivalent rotor slot opening,
y_{slot} is a local variable over a rotor slot; $y_{slot} \in (0,\ b_{sr})$.

An equivalent air-gap length $\delta_0(x,\varphi)$ can be locally determined for any rotor position angle φ. Then, it creates a function of two variables x and φ, which is periodic with respect to each of them.

The magnetic circuit is saturated mostly by the fundamental component of MMF. The idea to consider the magnetic stress in the stator and the rotor through a global increase of air-gap is well known method used in machine design process.

In the path of the resultant magnetic flux the stator and rotor cores are saturated and in the places where the main flux is crossing air-gap, the teeth are saturated. In standard machines teeth saturated first then cores because there a much higher flux density exist [18]. As a consequence saturation effects appear through a local reduction of magnetic permability of the iron paths and the substitutional air-gap should be modified. This modification consists of making the air-gap length a function of the MMF position and amplitude.
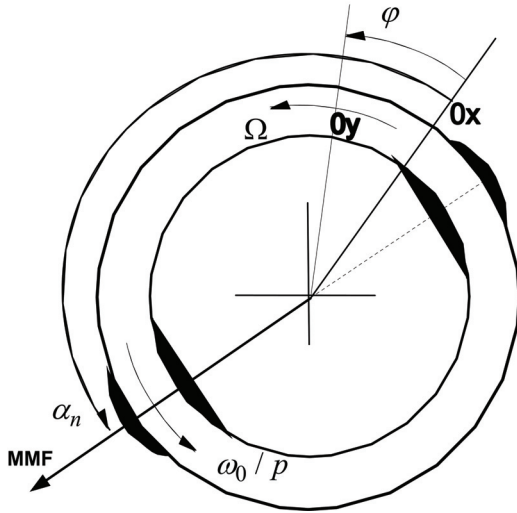
Fig. 5. Cross sectional view of saturated machine showing the variation of substitutional air-gap length

The degree of saturation can be obtained on the basis of saturation coefficient distributions $k_n(i_\mu, x, \alpha_n)$ determined by method magnetic field modelling [20]. This distribution of the saturation coefficient can be received directly by a comparison of distributions of the magnetic density in the air gap, for the cases where core is made with linear, relatively high permeability magnetic material and real non-linear material.

A typical air-gap variation, for instance, can be represented by following function of saturation coefficient

$$k_n(i_\mu, x, \alpha_n) = k_n^0(i_\mu) + k_n^2(i_\mu)\cos 2p(x - \alpha_n). \tag{11}$$

This coefficient depends on magnitude i_μ and location α_n of magnetizing current (MMF) and modifies the size of the smooth air-gap

$$\delta_c(x, \varphi, i_\mu, \alpha_n) = \delta_0(x, \varphi) + \Delta\delta_{sat}(i_\mu, x, \alpha_n), \tag{12}$$

where: $\Delta\delta_{sat}(i_\mu, x, \alpha_n) = (k_n(i_\mu, x, \alpha_n) - 1)\delta k_c$; $\delta = R - r$ and k_c – Carter coefficient.

On the basis of magnetic force line length in air-gap corrected by saturation coefficient, it is possible to obtain modified unitary function of air-gap permeance which take into account also slots and rotor eccentricity.

$$\Lambda(x, \varphi, i_\mu, \alpha_n) = \frac{1}{\delta_0(x, \varphi)k_n(i_\mu, x, \alpha_n)} = \frac{\Lambda_0(x, \varphi)}{k_n(i_\mu, x, \alpha_n)}, \tag{13}$$

where $\Lambda_0(x, \varphi)$ is a linear permeance function.

$$\Lambda_0(x, \varphi) = \frac{1}{\delta_0(x, \varphi)} = \sum_{m \in M}\sum_{n \in N}\Lambda_{m,n}\, e^{jmx}\, e^{jn\varphi}. \tag{14}$$

In this way nonlinear model of magnetic circuit can be transform to linear one.

It should be noted, that, when slotting on both sides of the air-gap is taken into account, the linear permeance function $\Lambda_0(x,\varphi)$ depends on two variables x and φ at any type of eccentricity and also for a symmetrically located rotor, whereas for the smooth air-gap the permeance function is constant for the symmetry case; for static and dynamic eccentricities it depends periodically on one variable and only for mixed eccentricity it becomes a function of two variables.

The Fourier coefficients $\Lambda_{m,n}$ can be obtained by the 2D FFT algorithm.

The inverse function of saturation coefficient

$$\frac{1}{k_n(i_\mu,x,\alpha_n)} = \sum_{k\in \mathrm{K}} C_k(i_\mu)\,e^{jk(x-\alpha_n)} \tag{15}$$

stems from the saturation effects.

If slotting and air-gap "deformations caused" saturations are taken into account, the permeance function depends on variables x, α_n, φ which is periodic with respect to each of them. This permeance function can be represented by the triple Fourier series

$$\Lambda(x,\varphi,i_\mu,\alpha_n) = \sum_{m\in \mathrm{M}} \sum_{n\in \mathrm{N}} \sum_{k\in \mathrm{K}} \Lambda_{m,n} C_k^*(i_\mu)\, e^{j(m-k)x}\, e^{jn\varphi}\, e^{jk\alpha_n}. \tag{16}$$

Generally, the air-gap is characterised by a permeance function and described by Fourier series in general form (12), where the $\mathrm{M}, \mathrm{N}, \mathrm{K}$ sets of m,n,k harmonics of permeance function contain successive whole numbers.

$$\mathrm{M} = \{-m_{max}\ldots-1,0,1\ldots m_{max}\}, \quad \mathrm{N} = \{-n_{max}\ldots-1,0,1\ldots n_{max}\}. \tag{17}$$

Set K relevant to saturation consist of only even harmonics

$$\mathrm{K} = \{-k_{max}\ldots-4p,-2p,0,2p,4p\ldots k_{max}\}. \tag{18}$$

3. Winding inductances accounting for rotor eccentricity

The formulas for all inductances can be enveloped from a general expression for inductances of two arbitrary coils 'a' and 'b' magnetizing non-uniform air-gap schematically show in Fig. 6.

Let these coils are represented by their MMFs and angular positions of their symmetry axes x_a and x_b. The MMFs of coils express by the Fourier series are done by the sets of harmonics order numbers $\mathrm{A} = \{-v_{max}\ldots-1,1\ldots v_{max}\}$ and $\mathrm{B} = \{-\rho_{max}\ldots-1,1\ldots \rho_{max}\}$ and winding factors $k_a^{|v|}$, $k_b^{|\rho|}$ of each harmonic [8].

The way of inductance determination for converters with two windings placed in non-uniform air-gap, assuming the occurrence of only radial field component, was presented in detail in paper [1]. This paper, however, did not concern the case when the function of air-gap permeance depends on three variables, therefore authors suggest a certain modification, thanks to which the function of inductance can be introduced.
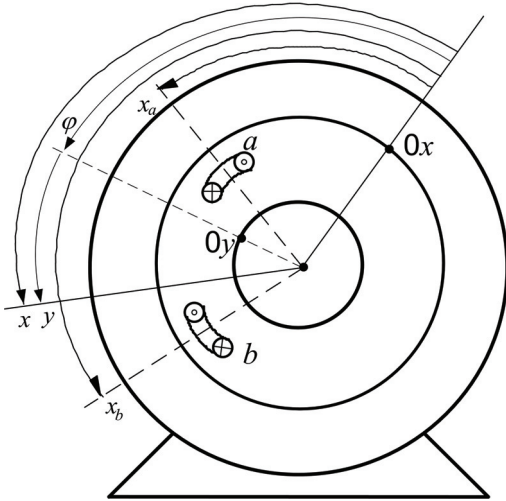
Fig. 6. Two coils magnetizing a air-gap

$$L_{ba} = \frac{2\mu_0 r_0}{\pi} \int\limits_{-l_c/2}^{l_c/2} \left\{ \sum_{v\in A} \sum_{m\in M} \sum_{k\in K} Q_1 W_a^{|v|} W_b^{|v+m-k|} \times \right.$$

$$\left. \times \left[\sum_{n_1\in N} \Lambda_{m,n_1} e^{jn_1\varphi} - Q_2 \frac{\sum\limits_{n_2\in N}\sum\limits_{n_3\in N} \Lambda_{-v,n_2}\Lambda_{v+m,n_3} e^{j(n_2+n_3)\varphi}}{\sum\limits_{n_4\in N} \Lambda_{0,n_4} e^{jn_4\varphi}} \right] C_k^*(i_\mu) e^{jv(x_b-x_a)} e^{j(m-k)x_b} e^{jka_n} \right\} dz. \tag{19}$$

In this expression l_c is an equivalent length of a machine core, $r_c = (R+r)/2$ is a mean radius air-gap, $W_a^{|v|} = w_a k_a^{|v|}/|v|$ and $W_b^{|v+m|} = w_b k_b^{|v+m|}/|v+m|$ are equivalent tern numbers, w_a and w_b are total tern numbers. Geometry of the air-gap is represented in (19) by an air-gap permeance function (16), which depends on a type of eccentricity.

Parameters Q_1 and Q_2 in (19) depend on the sets A, B, M, N and are defined as follow

$$Q_1 = \begin{cases} 1 \Leftrightarrow \forall v, \forall m, v\in A \wedge m\in M \wedge (-v-m+k)\in B \\ 0 \quad \text{for opposed condition}, \end{cases} \tag{20}$$

$$Q_2 = \begin{cases} 1 \Leftrightarrow Q_1 = 1 \wedge v\in M \wedge (-v-m+k)\in M \\ 0 \quad \text{for opposed condition}. \end{cases} \tag{21}$$

Generally, a mutual inductance L_{ba} is done by a quadruple Fourier series

$$L_{ba} = \sum_v \sum_m \sum_n \sum_k L_{v,m,n,k}^{ba} e^{jv(x_b-x_a)} e^{j(m-k)x_b} e^{jka_n} e^{jn\varphi}, \tag{22}$$

which in any case is reduced to the double Fourier series of rotation angles α_n and φ

$$L_{ba} = \sum_k \sum_l L_{k,l}^{ba} e^{jka_n} e^{jl\varphi}. \tag{23}$$

A self-inductance due to the main flux can be obtained putting $x_b = x_a$.

In order to determine all inductances of a 3-phase induction cage motor it has been assumed that stator phases produce MMFs with the odd harmonic of the orders $\pm p, \pm 3p, \pm 5p...$, the individual cage mash generates MMF containing all harmonics and the Fourier coefficients of MMF functions of windings can be found on classical way. Angels x_a and x_b have following forms [1]:

– inductances stator–stator

$$x_a = (a-1)\frac{2\pi}{3p} \qquad a = 1, 2, 3, \quad x_b = (b-1)\frac{2\pi}{3p}, \qquad b = 1, 2, 3, \tag{24}$$

– inductances rotor–rotor

$$x_a = (a-1)\frac{2\pi}{N} + \varphi, \quad a = 1, ..., N, \quad x_b = (b-1)\frac{2\pi}{N} + \varphi, \quad b = 1, ..., N, \tag{25}$$

– inductances rotor–stator

$$x_a = (a-1)\frac{2\pi}{3p}, \quad a = 1, 2, 3, \quad x_b = (b-1)\frac{2\pi}{N} + \varphi, \quad b = 1, ..., N. \tag{26}$$

Then formulas for self and mutual inductances can be expressed as:

– inductances stator–stator

$$L_{ba}^{ss} = \sum_v \sum_m \sum_n \sum_k L_{v,m,n,k}^{ss} \, e^{jv(b-a)\frac{2\pi}{3p}} \, e^{jm(b-1)\frac{2\pi}{3p}} \, e^{jn\varphi} \, e^{jk\alpha_n}, \tag{27}$$

– inductances rotor–rotor

$$L_{ba}^{rr} = \sum_v \sum_m \sum_n \sum_k L_{v,m,n,k}^{rr} \, e^{jv(b-a)\frac{2\pi}{N}} \, e^{jm(b-1)\frac{2\pi}{N}} \, e^{j(m+n)\varphi} \, e^{jk\alpha_n}, \tag{28}$$

– inductances rotor – stator

$$L_{ba}^{rs} = \sum_v \sum_m \sum_n \sum_k L_{v,m,n,k}^{rs} \, e^{jv[(b-1)\frac{2\pi}{N}-(a-1)\frac{2\pi}{3p}]} \, e^{jm(b-1)\frac{2\pi}{N}} \, e^{j(v+m+n)\varphi} \, e^{jk\alpha_n}. \tag{29}$$

A pseudo variation of the air gap length is assumed for modulation of linear function of permeance (14) according to saturation effects. The resultant inductance contains varying coefficients that are also a function of the saturation level represented by the saturation factor (11) [20].

4. Results of numerical tests

The main aim of tests is to illustrate the influence of eccentricity on the harmonic spectra of inductances.

All calculations in this paper have been done basing on the data of a motor SYJe132s, manufactured in a Polish factory, with rated data: $P_N = 2\,000$ kW, $n_N = 2\,980$ rpm, $U_N = 6$ kV, $I_N = 227$ A, having 42 open slots on the stator and $N = 36$ semi-close slots on the rotor, stator

radius $R = 0.2625$ m, rotor radius $r = 0.25965$ m, equivalent length of a machine core $l_c = 0.6$ m, number of stator windings $w_s = 70$.

For saturation illustration the exemplary calculations of the saturation coefficient have been done by FEM for this motor in Magnet software [20].
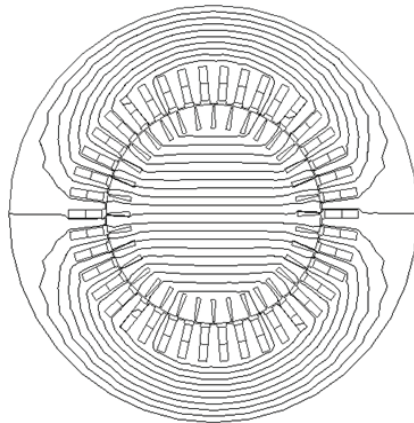

Fig. 7. Distribution of magnetic flux

The case with symmetrically situated rotor was taken into account. The distribution of saturation coefficient for nominal value of magnetizing current was approximated according to formula (11) [20] $k_n = 1.23 + 0.06 \cos(2(x - \alpha_n))$.

The distribution of the permeance functions $\Lambda_0(x,0) = 1/(\delta_0(x,0))$ for a motor with dynamic eccentricity $\varepsilon_d = 0.4$ and $\gamma_e = 0$ for half of period is shown in Fig. 8.
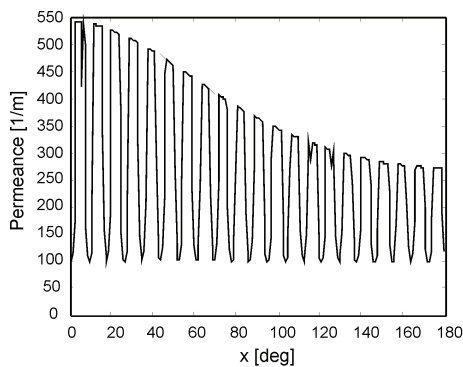

Fig. 8. Analytical calculation of distribution permeance function for dynamic eccentricity in situation $\gamma_e = 0$ (saturation neglected)
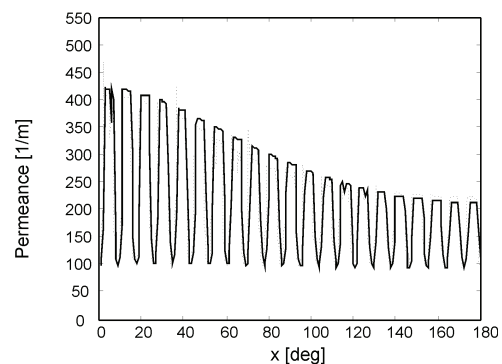
Fig. 9. Permeance function for dynamic eccentricity in situation $\gamma_e = 0$, $\alpha_n = 0$. Solid line – distribution obtained base on analytical formula (saturation considered); dashed line – distribution obtained based on FEM calculation [20]

Figure 9 presents waveforms of permeance function calculated based on analytical formula (14) and FEM. Figures 8 and 9 illustrate fact that essential point is taking into account magnetic stresses in iron of stator and rotor joke. For this such simple approach to the problem of saturation it shall be noted that the compatibility, both qualitative and quantitative, of the analytical waveform of the permeance function with the waveform obtained on the basis of the field calculations. It is clear that the analytical model predict the saturation with very good accuracy for case of rotor eccentricity and slotting presence.
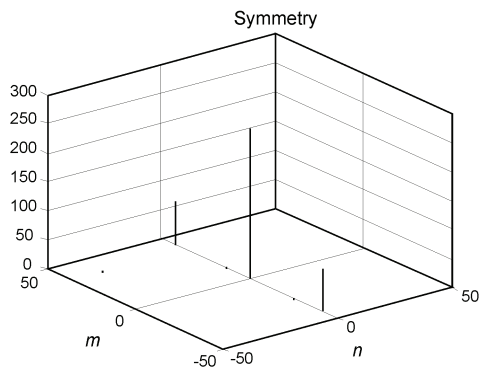

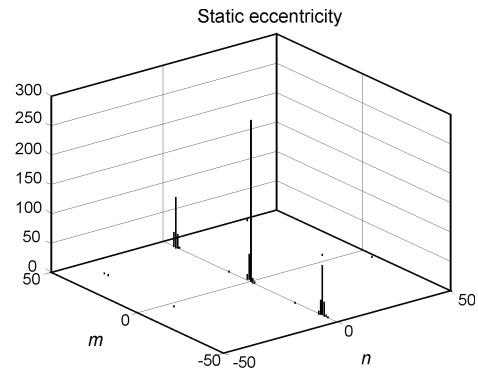Fig. 10a. Linear permeance function coefficients $\Lambda_{m,n}$ for symmetry

Fig. 10b. Linear permeance function coefficients $\Lambda_{m,n}$ for static eccentricity $\varepsilon_s = 0.4$
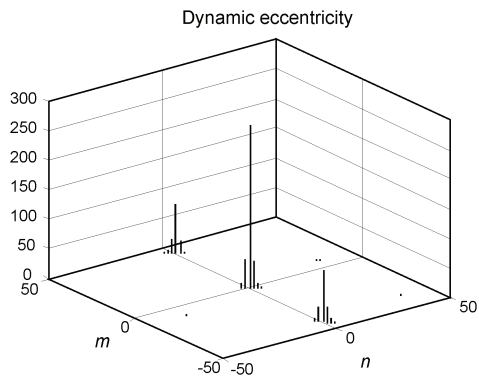

Fig. 10c. Linear permeance function coefficients $\Lambda_{m,n}$ for dynamic eccentricity $\varepsilon_d = 0.4$
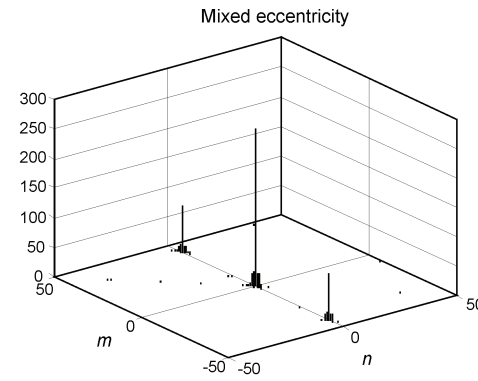

Fig. 10d. Linear permeance function coefficients $\Lambda_{m,n}$ for mixed eccentricity $\varepsilon_s = \varepsilon_d = 0.2$

In Figures 10a, b, c, d the changes of the spectrum of the 2D Fourier series of the linear permeance function for symmetry, static, dynamic and mixed eccentricity are shown. Computations have been done using the package MATLAB (dimensions of sets M and N were suitable to $m_{max} = n_{max} = 1021$).

It should be noted that rather high bars for harmonics 42 arise due to opened stator slots. It can be proved by comparison with a case of eccentricity when slotting is neglected (Fig. 11).
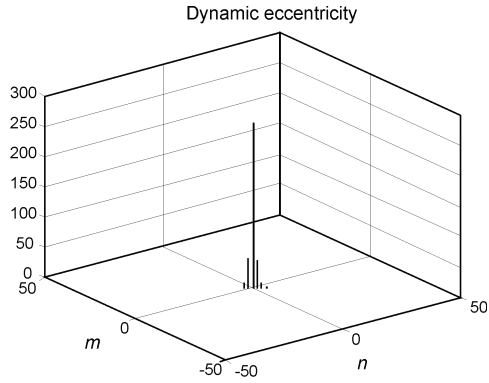
Fig. 11. Linear permeance function coefficients $\Lambda_{m,n}$ for static eccentricity $\varepsilon_s = 0.4$ (slotting neglected)

As we can see in the figures above the Fourier coefficients of the permeance function (Fig. 10) for particular eccentricities are spread in a way which is characteristic for the specific case. Shall the slotting not be taken into account, than for the symmetry state we would obtain only one point, for static eccentricity we would obtain only one column and for the dynamic eccentricity we would obtain only one diagonal (Fig. 11). The introduction of slotting gives additional characteristic harmonics and qualitatively brings the static and the dynamic eccentricities closer to the general case of the mixed eccentricity – the only difference is that the characteristic harmonics derived from the eccentricities calculated without slotting appear in the same places and at the same levels.
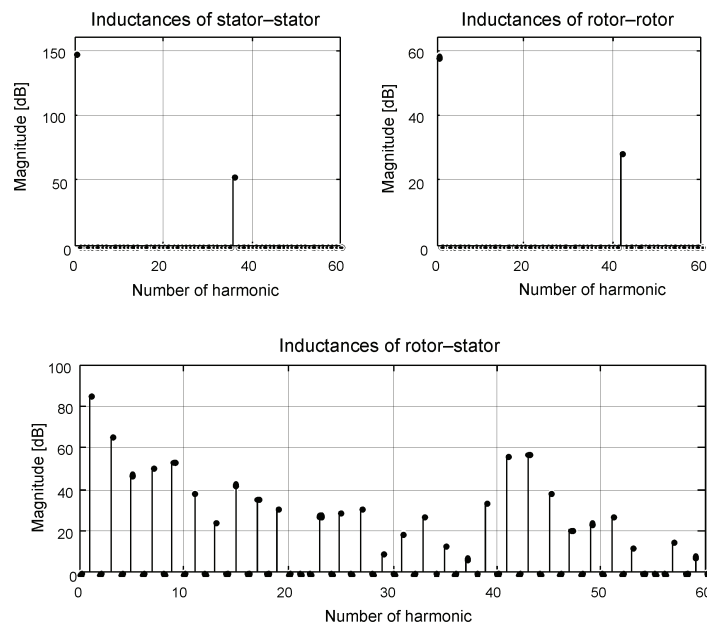

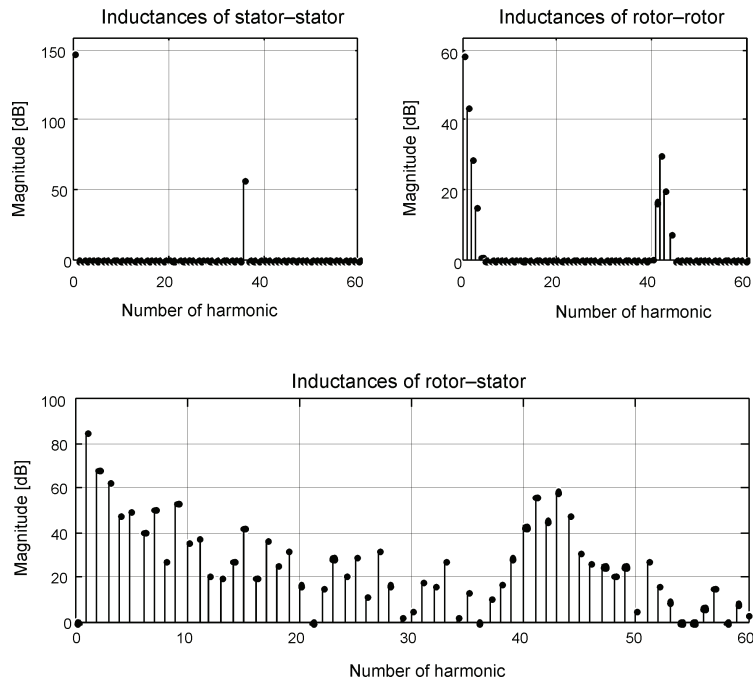Fig. 12a. Fourier spectrum of linear inductances (symmetry)

Inductances of stator–stator

Inductances of rotor–rotor

Inductances of rotor–stator

Fig. 12b. Fourier spectrum of linear inductances (static eccentricity $\varepsilon_s = 0.4$)

Inductances of stator–stator

Inductances of rotor–rotor
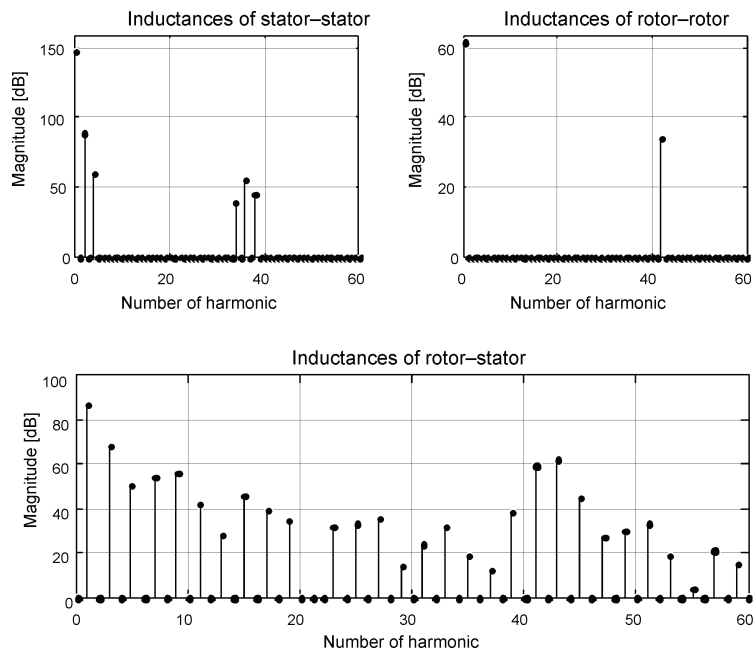
Inductances of rotor–stator

Fig. 12c. Fourier spectrum of linear inductances (dynamic eccentricity $\varepsilon_d = 0.4$)
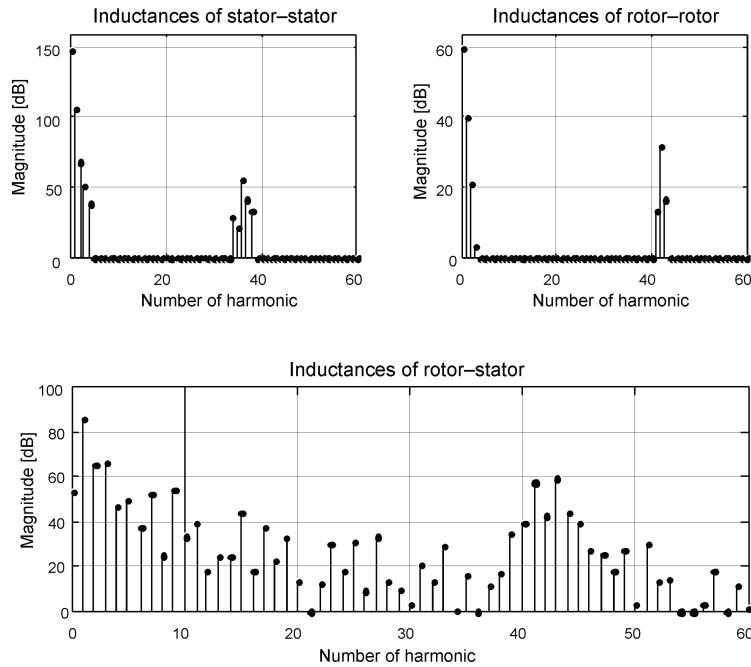
Fig. 12d. Fourier spectrum of linear inductances (mixed eccentricity $\varepsilon_s = \varepsilon_d = 0.2$)

The introduction of slotting gives additional characteristic harmonics around the slot harmonics in inductances, what significantly modifies the distribution of the Fourier inductance coefficients (Figs. 12). In Figs. 12a, b, c, d changes of the Fourier spectrum of inductances for cases of eccentricity for first phase of the stator with number 1 and first mesh of the rotor cage with number 1 are exemplary shown (in [dB] – ref. $1 \cdot 10^{-8}$ H, the number of MMF harmonics which were taken into account – 200).

These Figs. 12a-d present the distribution linear inductance coefficients magnitudes due to number of harmonics "*l*" according to formulas (27-29) for *k* = 0 (saturation neglected). Saturation effects modulate only this linear inductances according to inverse saturation coefficient (11).

5. Conclusions

In the paper, a specialized algorithm of inductance calculation for cage motors with eccentricity for diagnostics purpose has been extended on effects due to slotting on stator and rotor sides and saturation effects. The permeance function for such cases has been carefully studied. A comparison of permeances and inductances characterizing eccentricities has been done by numerical tests. Results showed that slotting introduce important changes to permeance functions especially not only quantitatively but also qualitatively. The saturation effects introduce

additional variation of the linear functions of permeance and inductances through the modulation by inverse function of saturation coefficient.

References

[1] T.J. Sobczyk, P. Drozdowski, *Inductances of electrical machine winding with a nonuniform air-gap*. Archiv fur Elektrotechnik 76: 213-218 (1993).

[2] A. Stavron, J. Penman, *The on-line quantification of air-gap eccentricity in induction machines*. Proc. of ICEM'94, Paris, 2: 261-266 (1994).

[3] F. Filippetti, G. Franceschini, C. Tassoni, P. Vas, *Broken bar detection in induction machines: comparison between current spectrum approach and parameter estimation approach*. IEEE 1994 Industry Applications Society Annual Meeting, Denver 1: 95-102 (1994).

[4] H.A. Toliyat, M.S. Arefeen, A.G. Parlos, *A Method for Dynamic Simulation of Air-Gap Eccentricity in Induction Machines*. IEEE Trans. on Industry Applications 32(4): 910-918 (1996).

[5] D.G. Dorrell, W.T. Thomson, S. Roach, *Analysis of airgap flux, current, and vibration signals as a function of the combination of static and dynamic airgap eccentricity in 3-phase induction motors*. IEEE Trans. on Industry Applications 33(1): 24-34 (1997).

[6] W.T. Thomson, A. Barbour, C. Tassoni, F. Filipetti, *An appraisal of the m.m.f. permeance method and finite element models to study static air gap eccentricity and its diagnosis in induction machines*. Proc. of ICEM'98, Istanbul 2182-2187 (1998).

[7] X. Tu, L.-A. Dessaint; M. El Kahel, A. O. Barry, *A New Model of Synchronous Machine Internal Faults Based on Winding Distribution*. Industrial Electronics, IEEE Transactions on 53(6): 1818-1828 (2006).

[8] A. Bellini, G. Franceschini, C. Tassoni, A. Toscani, *Assessment of induction machines rotor fault severity by different approaches*. 31st Conf. of IEEE IECON'05, Raleigh, North Carolina 1461-1466 (2005).

[9] S.D. Sudhoff, B.T. Kuhn, K.A. Corzine, B.T. Branecky, *Magnetic Equivalent Circuit Modeling of Induction Motors*. Energy Conversion, IEEE Transaction on 22: 259-270 (2007).

[10] S. Bachir, S. Tnani, J.-C. Trigeassou, G. Champenois, *Diagnosis by parameter estimation of stator and rotor faults occurring in induction machines*. Trans. on Industrial Electronics 53(3): 963-973 (2006).

[11] J.-H. Jung, J.-J. Lee, B.-H. Kwon, *Online Diagnosis of Induction Motors Using MCSA*. Industrial Electronics, IEEE Transactions on 53(6), 1842-1852 (2006).

[12] Xianghui Huang, T.G. Habetler, R.G. Harley, E.J. Wiedenbrug, *Using a Surge Tester to Detect Rotor Eccentricity Faults in Induction Motors, Industry Applications*. IEEE Transactions on 43(5), 1183-1190 (2007).

[13] Xiaodong Li, Qing Wu, S. Nandi, *Performance Analysis of a Three-Phase Induction Machine With Inclined Static Eccentricity*. Industry Applications, IEEE Transactions on 43(2): 531-541 (2007).

[14] B. Heller, V. Hamata, *Harmonic field effects in induction machines*. Elsevier Scientific Publishing, Oxford (1977).

[15] S. Nandi, S. Ahmed, H. Toliyat, *Detection of Rotor Slot and Other Eccentricity-Related Harmonics in a Three-Phase Induction Motor with Different Rotor Cages*. Power Engineering Review, IEEE 21(9): 62-62 (2001).

[16] S. Nandi, *Modeling of induction machines including stator and rotor slot effects*, Industry Applications, IEEE Trans on 40(4): 1058-1065 (2004).

[17] T.J. Sobczyk, K. Weinreb, T. Węgiel, M. Sułowicz, *Theoretical Study of Effects due to Rotor Eccentricities in Induction Motors*. Proc. of the 2nd IEEE SDEMPED'99, Gijon, 289-295 (1999).

[18] J.C. Moreira, T.A. Lipo, *Modeling of saturated AC machines including air gap flux harmonic components*. IEEE Trans. on Industry Applications 28(2): 343-349 (1992).

[19] T.J. Sobczyk, K. Weinreb, T. Wegiel, M. Sulowicz, A. Warzecha, *Effects in stator currents of cage motors due to saturation of main magnetic circuit*. Diagnostics for Electric Machines, Power Electronics and Drives, 2003. SDEMPED 2003. 4th IEEE International Symposium on 81-86 (2003).

[20] A. Warzecha, T. Węgiel, K. Weinreb, M. Sułowicz, *Non-Linear Permeance Function of Magnetic Circuit in Asynchronous Motor with Rotor Eccentricity.* Czasopismo Techniczne, Z.5-E/2005, Cracow University of Technology 87-100 (2005).

[21] S. Nandi, *A detailed model of induction machines with saturation extendable for fault analysis*. Industry Applications, IEEE Transactions on 40(5): 1302-1309 (2004).